TRANSPORT-EQUILIBRIUM SCHEMES FOR COMPUTING CONTACT DISCONTINUITIES IN TRAFFIC FLOW MODELING *

CHRISTOPHE CHALONS † AND PAOLA GOATIN ‡

Abstract. We present a very efficient numerical strategy for computing contact discontinuities in traffic flow modeling. We consider the Aw-Rascle model and the objective is to remove spurious oscillations generated for instance by the Godunov method near contact discontinuities. The method is mixed and based on both a random sampling strategy and the Godunov method. To prove the validity of the method, we show that it enjoys important stability properties and numerical tests are proposed. The convergence of the algorithm is demonstrated numerically.

Key words. Hyperbolic conservation laws, Continuous traffic models, Contact discontinuities, Transport-Equilibrium scheme.

subject classifications.

1. Introduction

Mathematical and numerical models for traffic dynamics can be developed under different approaches. We can distinguish between microscopic (particle based), mesoscopic (gas-kinetic) and macroscopic (fluid-dynamic) models. Here, we are interested in continuum models, which are based on conservation (or balance) equations. First-order models consist of one equation, describing the conservation of mass (i.e. the number of cars). The prototype of these models is due to Lighthill-Whitham [17] and Richards [20] (LWR). If another conservation equation is added, we obtain a so-called second-order model. A first prototype was proposed by Payne [19] and Whitham [24]. This kind of models mimics the isentropic Euler equations of fluid mechanics, requiring conservation of mass and momentum. However, traffic flow does not behave as usual fluids, and the Payne-Whitham model shows some absurdities, as pointed out by Daganzo [12]. In order to correct these drawbacks, Aw and Rascle [3] proposed another model, in which they replace the space derivative of the "pressure" in the momentum equation by the convective derivative $\partial_t + v\partial_x$, where v stands for the (mean) car velocity. More precisely, the model consists in a 2×2 system of conservation laws for the car density ρ and the "momentum" y which reads as follows:

$$\begin{cases} \partial_t \rho + \partial_x(\rho v) = 0, \\ \partial_t y + \partial_x(y v) = 0, \end{cases} \quad x\in\mathbb{R},\ t>0. \tag{1.1}$$

The conservative variable y is defined by

$$y = \rho w, \quad w = v + p(\rho). \tag{1.2}$$

Here p is a "pressure" term (as in gas dynamics) which takes into account drivers' reactions to the state of traffic in front of them. In this way, if we suitably choose the domain in the phase space, the model satisfies the basic principles:
- no information travels faster than cars;
- density and velocity remain non-negative and bounded.

*

†Université Denis Diderot-Paris 7 & Université Pierre et Marie Curie-Paris 6, UMR 7598 LJLL, Paris, F-75005 France, (chalons@math.jussieu.fr)

‡Laboratoire d'Analyse Non linéaire Appliquée et Modélisation, I.S.I.T.V., Université du Sud Toulon - Var, B.P. 56, 83162 La Valette du Var Cedex, France, (goatin@univ-tln.fr)

The velocity v is linked to the conservative unknown $\mathbf{u}=(\rho,y)$ by (1.2) and a closure relation for p. Following [3], the function p has to be chosen as a smooth and strictly increasing function such that $\rho p(\rho)$ is strictly convex. For instance, we will take (without any restriction) the following definition for the numerical experiments of this paper:

$$p(\rho)=v_{ref}\ln\left(\frac{\rho}{R}\right), \tag{1.3}$$

where R is the maximal car density allowed by the road, and v_{ref} is a given reference velocity. Introducing now three parameters v_M and w_m, w_M for the thresholds of v and w respectively, we define the following invariant region for (1.1) :

$$\Omega=\left\{(\rho,y)\in\mathbb{R}^2 \text{ with } \rho\in\left[0,R\right],\, v\in\left[0,v_M\right],\, w\in\left[w_m,w_M\right]\right\}. \tag{1.4}$$

We observe that (1.1) can also be written in condensed form as

$$\partial_t\mathbf{u}+\partial_x\mathbf{f}(\mathbf{u})=0, \qquad \mathbf{u}\in\Omega, \tag{1.5}$$

where the flux function $\mathbf{f}$ finds a clear definition from previous developments.

As detailed in Section 2, the system under consideration is strictly hyperbolic for $\rho>0$, with a genuinely nonlinear and a linearly degenerate characteristic field. The latter is associated with the faster eigenvalue which is equal to v and then develops discontinuous waves, the so-called contact discontinuities, for which the speed of propagation is continuous and given by v. In this paper, we will focus on the numerical approximation of these contact discontinuities.

In the past decade, the numerical approximation of contact discontinuities received a lot of attention in the context of compressible multicomponent (or multifluid) flows. Indeed, when the flow is made of several species, it is observed that classical conservative schemes (like Godunov's scheme) generate important nonphysical oscillations near the material fronts, eventually leading to numerical solutions that are not precise (at least for realistic meshes). The same pathologies also exist for single fluid computations, and they are going to appear for system (1.1). Several cures have been proposed in the literature, see for instance [15], [16], [1], [21], [13], [2], [4], ... and the references therein. Roughly speaking, the common idea is to keep on using a classical conservative scheme far from the material interfaces and to introduce a *non conservative* modification in the regions where the problem occurs, in order to preserve constant pressure and velocity. Note however that the threshold technique often attached to the local treatment prevents the methods from strictly preserving isolated contact discontinuities. The resulting *non conservative* schemes give good results and seem to be numerically converging. Note also that these strategies are usually designed for models involving at least two fluids, and then two pressure laws. As a consequence, it seems difficult to apply them to our "single fluid" system (1.1). We mention however that in [7], the authors will propose a mixed Lagrangian/Eulerian approach that applies also for closure relations involving a single pressure law.

Based on a recent work [5] (see also [6]) by the first author, we present in this paper an algorithm whose objective is to remove the spurious oscillations generated by the Godunov scheme (for instance) near the contact discontinuities of system (1.1). The method proposes to treat separately contact discontinuities using a random sampling strategy, and to keep on using the Godunov scheme for the other waves. As expected, the whole algorithm is *non conservative* but numerical experiments give very good numerical solutions with *sharp* (without numerical diffusion) contact discontinuities

and very small conservation errors, and show the numerical convergence. Moreover, we are able to prove that the method enjoys important stability properties like strong consistency and a maximum principle on the two Riemann invariants of system (1.1), see Theorems 3.1 and 3.2 in Section 3.3. Note also that our algorithm is free of threshold techniques. As a consequence of all these properties, contact discontinuities are *always* computed without oscillations.

To conclude this section, we recall that another second-order model has been proposed by Colombo [10], and also this model has a genuinely nonlinear and a linearly degenerate field. Then, the same difficulties related to the numerical contact discontinuities are expected to occur. Moreover, both models [10, 3] have been coupled with the LWR equation, giving origin to traffic flow models with phase transitions [11, 14]. The techniques presented in this paper can be easily adapted and used in these cases. In particular, for models with phase transitions, an efficient numerical scheme has been proposed by the authors in [8]. It can be combined with the present one in order to better approximate contact discontinuities.

2. Basic properties of the Aw-Rascle model

In this section, we briefly recall the basic features of the model under consideration and we refer the reader to [3] (see also [14]) for more details, knowing that the properties here stated follow from usual considerations. The basic informations on the Aw-Rascle system are collected in the following table:

$$\begin{array}{ll}
r_1(\rho,v)=\begin{bmatrix}1\\ -p'(\rho)\end{bmatrix}, & r_2(\rho,v)=\begin{bmatrix}1\\ 0\end{bmatrix},\\
\lambda_1(\rho,v)=v-\rho p'(\rho), & \lambda_2(\rho,v)=v,\\
\nabla\lambda_1\cdot r_1=-2p'(\rho)-\rho p''(\rho), & \nabla\lambda_2\cdot r_2=0,\\
\mathcal{L}_1(\rho;\rho_o,v_o)=v_o+p(\rho_o)-p(\rho), & \mathcal{L}_2(\rho;\rho_o,v_o)=v_o,\\
w_1=v+p(\rho), & w_2=v,
\end{array} \tag{2.1}$$

where r_i is the i-th right eigenvector, λ_i the corresponding eigenvalue and $\mathcal{L}_i$ is the i-Lax curve. We note that shock and rarefaction curves coincide, hence the system belongs to the Temple class [23]. The Riemann invariants associated with each eigenvalue λ_1 and λ_2 are $w_1=v+p(\rho)$ and $w_2=v$ respectively. In addition, it is easily seen that the first characteristic field is genuinely nonlinear, and the second is linearly degenerate. Therefore, depending on the initial data, the self-similar solution to the general Riemann problem

$$\begin{cases}\partial_t\mathbf{u}+\partial_x\mathbf{f}(\mathbf{u})=0,\\ \mathbf{u}(x,0)=\begin{cases}\mathbf{u}^l \text{ if } x<0,\\ \mathbf{u}^r \text{ if } x>0,\end{cases}\end{cases} \tag{2.2}$$

will be made of one Lax wave (shock or rarefaction) moving with negative and/or positive speeds, and a contact discontinuity always moving with positive speed v. For a more detailed description of the Riemann solver see again [3]. Using the Riemann coordinates and the property that w_1 (respectively w_2) is constant across the waves of the first (respectively second) family, the intermediate state $\mathbf{u}^\star(\mathbf{u}^l,\mathbf{u}^r)$ in the Riemann solution is easily computed :

$$\begin{cases}w_1^\star=w_1^l=v^l+p(\rho^l),\\ w_2^\star=w_2^r=v^r,\end{cases} \quad\Longrightarrow\quad \begin{cases}\rho^\star=\rho^l\exp\left(\dfrac{v^l-v^r}{v_{ref}}\right),\\ y^\star=\rho^\star(v^r+p(\rho^\star)).\end{cases}$$

Of course, we note that $v^\star := v(\mathbf{u}^\star(\mathbf{u}^l,\mathbf{u}^r)) = v^r$. We will use the above cheap computation in our algorithm. On the contrary, we will not compute directly rarefaction waves.
It is also important for the forthcoming developments to notice that the solution to (2.2) obeys a maximum principle on the two Riemann invariants. In other words, if $(x,t) \to \mathbf{u_r}(\frac{x}{t};\mathbf{u}^l,\mathbf{u}^r)$ denotes the self-similar solution of (2.2), we have

$$\begin{cases} \inf\{v^l+p(\rho^l), v^r+p(\rho^r)\} \le (v+p)\left(\mathbf{u_r}\left(\dfrac{x}{t};\mathbf{u}^l,\mathbf{u}^r\right)\right) \le \sup\{v^l+p(\rho^l), v^r+p(\rho^r)\}, \\ \inf\{v^l, v^r\} \le v\left(\mathbf{u_r}\left(\dfrac{x}{t};\mathbf{u}^l,\mathbf{u}^r\right)\right) \le \sup\{v^l, v^r\}. \end{cases}$$

3. Numerical approximation

We first briefly recall the Godunov scheme applied to system (1.1), showing that it introduces nonphysical oscillations near contact discontinuities, which can significantly affect the whole approximate solution. To overcome this problem, we will introduce a new method in which we make evolve separately the contact discontinuities and the shock or rarefaction waves.

Let Δx and Δt be two constant increments for space and time discretizations, and $\nu = \Delta t/\Delta x$. We then define the mesh interfaces $x_{j+1/2} = j\Delta x$ and the cell centers $x_j = (j+1/2)\Delta x$ for $j \in \mathbb{Z}$, the intermediate times $t^n = n\Delta t$ for $n \in \mathbb{N}$, and at each time t^n we denote $\mathbf{u}_j^n$ an approximate mean value of the solution of (1.5) on the interval $\mathcal{C}_j = [x_{j-1/2}, x_{j+1/2})$, $j \in \mathbb{Z}$. In other words, a piecewise constant approximation $x \to \mathbf{u}_\nu(x,t^n)$ of the solution $\mathbf{u}$ is given by

$$\mathbf{u}_\nu(x,t^n) = \mathbf{u}_j^n \text{ for all } x \in \mathcal{C}_j,\ j \in \mathbb{Z},\ n \in \mathbb{N}.$$

When $n = 0$, we set

$$\mathbf{u}_j^0 = \frac{1}{\Delta x}\int_{x_{j-1/2}}^{x_{j+1/2}} \mathbf{u}_0(x)dx, \text{ for all } j \in \mathbb{Z}, \tag{3.1}$$

where $\mathbf{u}_0 \in \Omega$ is a given initial data.

Assuming as given a sequence $(\mathbf{u}_j^n)_{j\in\mathbb{Z}}$ at time t^n, we concentrate now on the computation of an approximate solution at the next time level t^{n+1}.

3.1. The Godunov scheme

As it is well-known, Godunov scheme writes as follows

$$\mathbf{u}_j^{n+1} = \mathbf{u}_j^n - \frac{\Delta t}{\Delta x}(\mathbf{f}_{j+1/2}^n - \mathbf{f}_{j-1/2}^n) \text{ for all } j \in \mathbb{Z}, \tag{3.2}$$

where the numerical fluxes are such that

$$\mathbf{f}_{j+1/2}^n = \mathbf{f}(\mathbf{u_r}(0^-;\mathbf{u}_j^n,\mathbf{u}_{j+1}^n)) \text{ for all } j \in \mathbb{Z}. \tag{3.3}$$

Let $\mathbf{v}$ be the solution for times $t \in [0,\Delta t]$ of (1.1) with piecewise constant initial data $\mathbf{u}_0(x) = \mathbf{u}_\nu(x,t^n)$. Under the usual CFL restriction

$$\frac{\Delta t}{\Delta x}\max_{\mathbf{u}}\{|\lambda_i(\mathbf{u})|,\ i=1,2\} \le \frac{1}{2} \tag{3.4}$$

for all the $\mathbf{u}$ under consideration, $\mathbf{v}$ is obtained by gluing together the solutions of the Riemann problems set at each interface. More precisely

$$\mathbf{v}(x,t) = \mathbf{u_r}\left(\frac{x-x_{j+1/2}}{t};\mathbf{u}_j^n,\mathbf{u}_{j+1}^n\right) \text{ for all } (x,t) \in [x_j,x_{j+1}]\times[0,\Delta t]. \tag{3.5}$$

See Figure 3.1 for an illustration. Green's formula tells us that (3.2) is equivalent to average the function $x \to \mathbf{v}(x,\Delta t)$ on the interval $[x_{j-1/2},x_{j+1/2}]$:

$$\mathbf{u}_j^{n+1} = \frac{1}{\Delta x}\int_{x_{j-1/2}}^{x_{j+1/2}} \mathbf{v}(x,\Delta t)dx,\ j\in\mathbb{Z}. \tag{3.6}$$

Another equivalent way to recover (3.2) consists in setting

$$\mathbf{u}_j^{n+1} = \frac{1}{2}(\mathbf{u}_{j+1/2,L}^{n+1} + \mathbf{u}_{j-1/2,R}^{n+1}), \tag{3.7}$$

where

$$\mathbf{u}_{j+1/2,L}^{n+1} = \frac{2}{\Delta x}\int_{x_j}^{x_{j+1/2}} \mathbf{u_r}\left(\frac{x-x_{j+1/2}}{\Delta t};\mathbf{u}_j^n,\mathbf{u}_{j+1}^n\right)dx = \mathbf{u}_j^n - \frac{2\Delta t}{\Delta x}(\mathbf{f}_{j+1/2}^n - \mathbf{f}(\mathbf{u}_j^n)) \tag{3.8}$$

and

$$\mathbf{u}_{j+1/2,R}^{n+1} = \frac{2}{\Delta x}\int_{x_{j+1/2}}^{x_{j+1}} \mathbf{u_r}\left(\frac{x-x_{j+1/2}}{\Delta t};\mathbf{u}_j^n,\mathbf{u}_{j+1}^n\right)dx = \mathbf{u}_{j+1}^n - \frac{2\Delta t}{\Delta x}(\mathbf{f}(\mathbf{u}_{j+1}^n) - \mathbf{f}_{j+1/2}^n) \tag{3.9}$$

denotes the averages of the Riemann solution $x \to \mathbf{u_r}\left(\frac{x-x_{j+1/2}}{\Delta t};\mathbf{u}_j^n,\mathbf{u}_{j+1}^n\right)$ on the half-cells $[x_j,x_{j+1/2}]$ and $[x_{j+1/2},x_{j+1}]$. This point of view will be useful in the following.

3.2. Failure of Godunov scheme in properly capturing contact discontinuities

Let us consider the Riemann problem (2.2) with $\mathbf{u}^l = (\rho^l,y^l)$ and $\mathbf{u}^r = (\rho^r,y^r)$ such that $\rho^l > 0$, $\rho^r > 0$, $\rho^l \neq \rho^r$ but $v^l = v^r$. In this case, the solution simply consists in a contact discontinuity propagating at speed $v_0 := v^l = v^r$:

$$\mathbf{u}(x,t) = \begin{cases} \mathbf{u}^l \text{ if } x < v_0 t, \\ \mathbf{u}^r \text{ if } x > v_0 t. \end{cases}$$

From now on, we assume $v_0 > 0$.

What happens in the first time step ?

From (3.1) we have that

$$\mathbf{u}_j^0 = \begin{cases} \mathbf{u}^l \text{ if } j \leq 0, \\ \mathbf{u}^r \text{ if } j > 0. \end{cases}$$

Due to the CFL restriction (3.4) and the property $v_0 > 0$, only the cell $\mathcal{C}_1$ may be affected by update formula (3.6) in the first time step. In other words,

$$\mathbf{u}_j^1 = \mathbf{u}_j^0 \quad \text{for all} \quad j \neq 1.$$

For $j = 1$, (3.6) is equivalent to

$$\rho_1^1 = \overline{\rho} \quad \text{and} \quad y_1^1 = \overline{y},$$

where we have used the notation

$$\overline{\alpha} = \frac{1}{\Delta x}\int_0^{\Delta x} \alpha(x,\Delta t)dx.$$

We observe that

$$\overline{y} = \frac{1}{\Delta x}\int_0^{\Delta x} y(x,\Delta t)dx = \frac{1}{\Delta x}\int_0^{\Delta x} (\rho v + \rho p(\rho))(x,\Delta t)dx.$$

Since the velocity remains constant across a contact discontinuity, we have

$$\overline{y} = v_0 \frac{1}{\Delta x}\int_0^{\Delta x} \rho(x,\Delta t)dx + \frac{1}{\Delta x}\int_0^{\Delta x} (\rho p(\rho))(x,\Delta t)dx = v_0\overline{\rho} + \overline{\rho p(\rho)}.$$

On the contrary, if we calculate v_1^1 from $\overline{\rho}$ and $\overline{y}$, we get

$$v_1^1 = \frac{\overline{y}}{\overline{\rho}} - p(\overline{\rho}) = v_0 + \frac{\overline{\rho p(\rho)} - \overline{\rho} p(\overline{\rho})}{\overline{\rho}}.$$

We observe that the function $\rho \to \rho p(\rho)$ is convex. By Jensen's inequality, we deduce $\overline{\rho p(\rho)} \geq \overline{\rho} p(\overline{\rho})$ and then

$$v_1^1 \geq v_0,$$

with strict inequality generally speaking. Which means that after the first time iteration, the velocity no longer equals v_0 everywhere. We conclude that the Godunov method is not able to keep constant the velocity profile and then to properly capture contact discontinuities. In Section 4, we will show that the non physical values created by the Godunov method around contact discontinuities may significantly damage the numerical solution. Our goal is to design a suitable algorithm to remove these spurious values.

Remark 1. (i) The failure we have just underlined is due to the fact that Godunov method does not obey to a maximum principle property on the velocity v. The algorithm we propose in the next section verifies the maximum principle on the Riemann invariants v and $v+p(\rho)$, see Theorem 3.2.
(ii) It is important to notice that if we now consider an isolated 1-wave between $\mathbf{u}^l$ and $\mathbf{u}^r$, the Godunov method actually keeps constant the Riemann invariant $v+p(\rho)$. If we set $C_0 := v^l + p(\rho^l) = v^r + p(\rho^r)$, we have indeed

$$(v+p(\rho))_1^1 = (\frac{y}{\rho})_1^1 = \frac{\overline{y}}{\overline{\rho}} = \frac{\overline{\rho(v+p(\rho))}}{\overline{\rho}} = C_0\frac{\overline{\rho}}{\overline{\rho}} = C_0.$$

This property is very interesting and means in particular that all the points in a numerical 1-wave profile associated with Godunov's method belong to the same 1-wave curve for all the possible choices of $p(\rho)$. This property is also satisfied by our new method (see Theorem 3.1 (iii) and Theorem 3.2).

3.3. A Transport-Equilibrium scheme

We propose now an algorithm that allows to avoid the spurious oscillations generated near the contact discontinuities by the classical Godunov method. The basic idea is to treat in a different way contact discontinuities on one side, and other waves (shock and rarefaction waves) on the other side. We will keep on using Godunov method for shocks and rarefactions (since it works well and is conservative), and we will propose a particular treatment for contact discontinuities, which make use of a (Glimm's) random sampling strategy.

We set

$$\mathbf{g}(\mathbf{u}^l, \mathbf{u}^r) = \mathbf{f}(\mathbf{u_r}(0^-; \mathbf{u}^l, \mathbf{u}^r)),$$

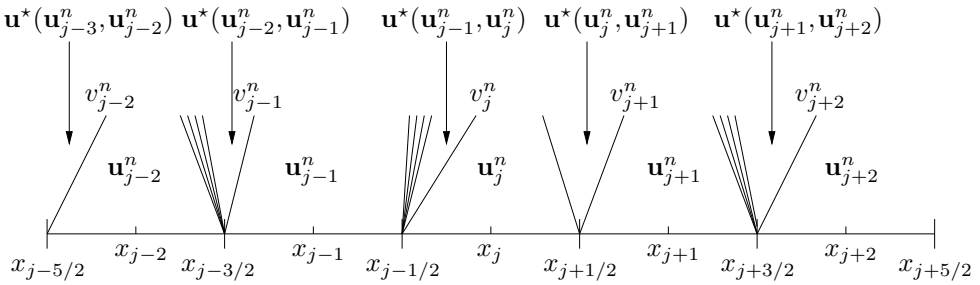

FIG. 3.1. *Illustration of the notations used in the paper.*

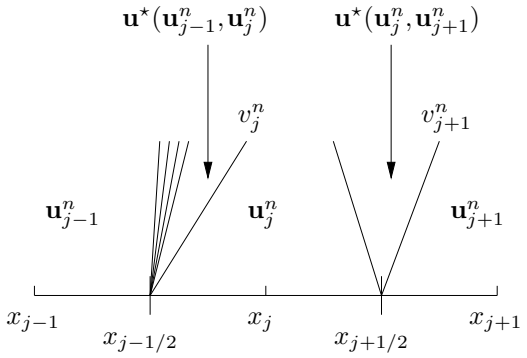

FIG. 3.2. *Restriction on the interval* (x_{j-1},x_{j+1}).

so that the numerical flux of the Godunov method writes $\mathbf{f}^n_{j+1/2}=\mathbf{g}(\mathbf{u}^n_j,\mathbf{u}^n_{j+1})$ for all $j\in\mathbb{Z}$. Recall that $\mathbf{u}^\star(\mathbf{u}^l,\mathbf{u}^r)$ is the intermediate state in the Riemann solution $\mathbf{u_r}(.;\mathbf{u}^l,\mathbf{u}^r)$ (between the 1-wave and the 2-contact discontinuity), so that $\mathbf{u}^l$ and $\mathbf{u}^\star(\mathbf{u}^l,\mathbf{u}^r)$ are connected by a 1-wave and $\mathbf{u}^\star(\mathbf{u}^l,\mathbf{u}^r)$ and $\mathbf{u}^r$ are connected by a 2-contact discontinuity. Of course, we have $\mathbf{u}^\star(\mathbf{u}^l,\mathbf{u}^r)=\mathbf{u}^r$ (respectively $\mathbf{u}^\star(\mathbf{u}^l,\mathbf{u}^r)=\mathbf{u}^l$) if $\mathbf{u}^l$ and $\mathbf{u}^r$ are connected by a 1-wave (respectively a 2-contact discontinuity), and we set $\mathbf{u}^\star(\mathbf{u},\mathbf{u})=\mathbf{u}$ for all $\mathbf{u}$. See Figure 3.1.

The method is made of two steps. On each interval $[x_j,x_{j+1}]$, $j\in\mathbb{Z}$, the first step takes into account only the contact discontinuity in the Riemann solution $\mathbf{u_r}(.;\mathbf{u}^n_j,\mathbf{u}^n_{j+1})$, while the second step focuses on the 1-wave. Our procedure may be viewed as a waves splitting strategy, performed locally around each interface $x_{j+1/2}$ where a Riemann problem is set.

Assuming as given $\mathbf{u}^n_{j-1}$, $\mathbf{u}^n_j$ and $\mathbf{u}^n_{j+1}$, we show now how to define $\mathbf{u}^{n+1}_j$. Note that, under the CFL condition (3.4), it is sufficient to focus on the interval $[x_{j-1},x_{j+1}]$, since the Riemann problems set at other interfaces are not expected to influence the definition of $\mathbf{u}^{n+1}_j$. See below Figure 3.2.

Step 1 : Propagation of contact discontinuities ($t^n\to t^{n+1/2}$)

In this step, we focus on the dynamics of contact discontinuities. We proceed as follows. The Riemann problems at interfaces $x_{j-1/2}$ and $x_{j+1/2}$ generally develop a 1-wave and a 2-contact discontinuity, the latter propagating at speed v^n_j and v^n_{j+1} respectively (see again Figure 3.2). These velocities being nonnegative, the contact discontinuities only affect $[x_{j-1/2},x_j)$ and $[x_{j+1/2},x_{j+1}]$, but not $[x_{j-1},x_{j-1/2})$ and

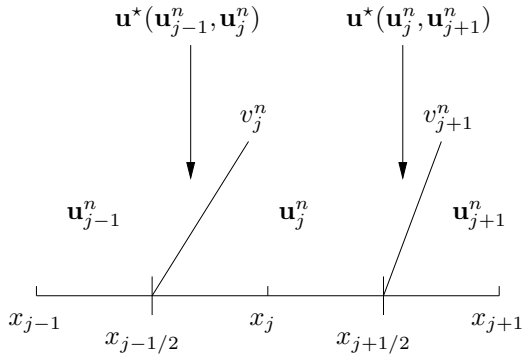

FIG. 3.3. *Function* $\tilde{\mathbf{v}}$.

$[x_j,x_{j+1/2})$. This means that the Riemann solutions $\mathbf{u_r}(.;\mathbf{u}^n_{j-1},\mathbf{u}^n_j)$ and $\mathbf{u_r}(.;\mathbf{u}^n_j,\mathbf{u}^n_{j+1})$ could be replaced in this step with the following function

$$\tilde{\mathbf{v}}(x,t)=\begin{cases}\mathbf{u}^n_{j-1} \text{ if } x\in[x_{j-1},x_{j-1/2})\\ \mathbf{u}^\star(\mathbf{u}^n_{j-1},\mathbf{u}^n_j) \text{ if } x\in[x_{j-1/2},x_{j-1/2}+v^n_j(t-t^n))\\ \mathbf{u}^n_j \text{ if } x\in[x_{j-1/2}+v^n_j(t-t^n),x_{j+1/2})\\ \mathbf{u}^\star(\mathbf{u}^n_j,\mathbf{u}^n_{j+1}) \text{ if } x\in[x_{j+1/2},x_{j+1/2}+v^n_{j+1}(t-t^n))\\ \mathbf{u}^n_{j+1} \text{ if } x\in[x_{j+1/2}+v^n_{j+1}(t-t^n),x_{j+1}]\end{cases}$$

on the whole interval (x_{j-1},x_{j+1}), see Figure 3.3. Of course, this function has to be considered as a substitute of function $\mathbf{v}$ in (3.5), where only contact discontinuities have been kept.

In order to properly capture contact discontinuities, we propose to define $\tilde{\mathbf{v}}(x,t^{n+1/2})$ as a piecewise constant function on each interval $[x_{j-1},x_{j-1/2})$, $[x_{j-1/2},x_{j+1/2})$ and $[x_{j+1/2},x_{j+1}]$ (as $\tilde{\mathbf{v}}(x,t^n)$ is) by means of a Glimm's random sampling strategy. More precisely, we pick up randomly on the cell $[x_{j-1},x_{j+1}]$ a value between $\mathbf{u}^n_{j-1}$, $\mathbf{u}^\star(\mathbf{u}^n_{j-1},\mathbf{u}^n_j)$, $\mathbf{u}^n_j$, $\mathbf{u}^\star(\mathbf{u}^n_j,\mathbf{u}^n_{j+1})$ and $\mathbf{u}^n_{j+1}$ in agreement with their rate of presence in the corresponding interval, or equivalently in agreement with the definition of the function $x\to\tilde{\mathbf{v}}(x,t^n+\Delta t)$. Given a well distributed random sequence (a_n) within interval $(0,1)$, it amounts to set :

$$\tilde{\mathbf{v}}(x,t^{n+1/2})=\begin{cases}\mathbf{u}^n_{j-1} \text{ if } x\in[x_{j-1},x_{j-1/2})\\ \mathbf{u}^{n+1/2}_j \text{ if } x\in[x_{j-1/2},x_{j+1/2})\\ \mathbf{u}^{n+1/2}_{j+1,L} \text{ if } x\in[x_{j+1/2},x_{j+1}]\end{cases}$$

with

$$\mathbf{u}^{n+1/2}_j=\begin{cases}\mathbf{u}^\star(\mathbf{u}^n_{j-1},\mathbf{u}^n_j) \text{ if } & a_{n+1}\in(0,\frac{\Delta t}{\Delta x}v^n_j),\\ \mathbf{u}^n_j \text{ if } & a_{n+1}\in[\frac{\Delta t}{\Delta x}v^n_j,1),\end{cases}\tag{3.10}$$

and

$$\mathbf{u}^{n+1/2}_{j+1,L}=\begin{cases}\mathbf{u}^\star(\mathbf{u}^n_j,\mathbf{u}^n_{j+1}) \text{ if } & a_{n+1}\in(0,\frac{2\Delta t}{\Delta x}v^n_j),\\ \mathbf{u}^n_{j+1} \text{ if } & a_{n+1}\in[\frac{2\Delta t}{\Delta x}v^n_j,1).\end{cases}\tag{3.11}$$

See Figure 3.4. In practice, we will consider the well-known van der Corput random

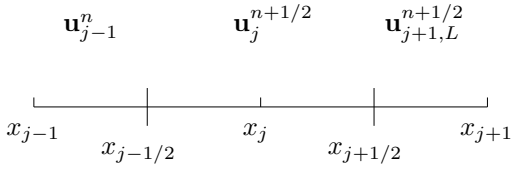

FIG. 3.4. *Function* $\tilde{\mathbf{v}}(x,t^{n+1/2})$.

sequence (a_n) defined by

$$a_n = \sum_{k=0}^{m} i_k 2^{-(k+1)},$$

where $n = \sum_{k=0}^{m} i_k 2^k$, $i_k = 0,1$, denotes the binary expansion of the integers $n = 1,2,...$ (see for instance Collela [9]).

Remark 2. It is worth noticing from now on that if both $\mathbf{u}_{j-1}^n$ and $\mathbf{u}_j^n$ on one hand and $\mathbf{u}_j^n$ and $\mathbf{u}_{j+1}^n$ on the other hand can be connected by a 1-wave, then $\mathbf{u}^\star(\mathbf{u}_{j-1}^n, \mathbf{u}_j^n) = \mathbf{u}_j^n$ and $\mathbf{u}^\star(\mathbf{u}_j^n, \mathbf{u}_{j+1}^n) = \mathbf{u}_{j+1}^n$ and as an immediate consequence of (3.10)-(3.11), $\tilde{\mathbf{v}}(x,t^{n+1/2}) = \tilde{\mathbf{v}}(x,t^n)$. Then, the first step is transparent when no contact discontinuity is present.

Step 2 : Account for the dynamics of shock and rarefaction waves ($t^{n+1/2} \to t^{n+1}$) Let us now concentrate on the parts of the solution located on the left and on the right of the contact discontinuities.

Let us first consider the Riemann problem set at the interface $x_{j+1/2}$ for which only the part of the solution located on the left of the contact discontinuity may enter the cell $\mathcal{C}_j = [x_{j-1/2}, x_{j+1/2})$. See Figure 3.2. We propose to take it into account by simply averaging $\mathbf{u_r}(.;\mathbf{u}_j^{n+1/2}, \mathbf{u}_{j+1,L}^{n+1/2})$ on $(x_j, x_{j+1/2})$ as in (3.8). Note that the restrictions to $[x_j, x_{j+1/2})$ of $\mathbf{u_r}(.;\mathbf{u}_j^{n+1/2}, \mathbf{u}_{j+1,L}^{n+1/2})$ and $\mathbf{u_r}(.;\mathbf{u}_j^{n+1/2}, \mathbf{u}_{j+1}^n)$ are the same since $\mathbf{u}_{j+1,L}^{n+1/2}$ and $\mathbf{u}_{j+1}^n$ are either equal or separated by a contact discontinuity. Then we set

$$\begin{aligned} \mathbf{u}_{j+1/2,L}^{n+1} &= \frac{2}{\Delta x} \int_{x_j}^{x_{j+1/2}} \mathbf{u_r}\left(\frac{x - x_{j+1/2}}{\Delta t}; \mathbf{u}_j^{n+1/2}, \mathbf{u}_{j+1}^n\right) dx \\ &= \mathbf{u}_j^{n+1/2} - \tfrac{2\Delta t}{\Delta x}(\mathbf{g}(\mathbf{u}_j^{n+1/2}, \mathbf{u}_{j+1}^n) - \mathbf{f}(\mathbf{u}_j^{n+1/2})). \end{aligned} \tag{3.12}$$

Let us now focus on the Riemann problem set at the interface $x_{j-1/2}$ for which both parts of the solution located on the left and on the right of the contact discontinuity may enter the cell $\mathcal{C}_j$ depending on the sense of propagation of the 1-wave (see again Figure 3.2). There are two possibilities:

• $\mathbf{u}_j^{n+1/2} = \mathbf{u}_j^n$: it corresponds to the situation where the random sampling "decided" that the (possibly present) contact discontinuity of $\mathbf{u_r}(.;\mathbf{u}_{j-1}^n, \mathbf{u}_j^n)$ do not yet enter the cell $\mathcal{C}_j$. Then we only have to account for:

- the right part of the contact discontinuity in $\mathbf{u_r}(.;\mathbf{u}_{j-1}^n, \mathbf{u}_j^n)$ (*i.e.* $\mathbf{u}_j^n = \mathbf{u}_j^{n+1/2}$) *if a contact discontinuity is actually present* in $\mathbf{u_r}(.;\mathbf{u}_{j-1}^n, \mathbf{u}_j^n)$, that is if $\mathbf{u}^\star(\mathbf{u}_{j-1}^n, \mathbf{u}_j^n) \neq \mathbf{u}_j^n$. This is simply done by replacing $\mathbf{u}_{j-1}^n$ and $\mathbf{u}_j^n$ with $\mathbf{u}_j^{n+1/2} = \mathbf{u}_j^n$ in $\mathbf{u_r}(.;\mathbf{u}_{j-1}^n, \mathbf{u}_j^n)$;
- the part of the solution $\mathbf{u_r}(.;\mathbf{u}_{j-1}^n, \mathbf{u}_j^n)$ entering $\mathcal{C}_j$ *if no contact discontinuity is present* in $\mathbf{u_r}(.;\mathbf{u}_{j-1}^n, \mathbf{u}_j^n)$, that is if $\mathbf{u}^\star(\mathbf{u}_{j-1}^n, \mathbf{u}_j^n) = \mathbf{u}_j^n$.

• $\mathbf{u}_j^{n+1/2}=\mathbf{u}^\star(\mathbf{u}_{j-1}^n,\mathbf{u}_j^n)\neq\mathbf{u}_j^n$: it corresponds to the situation where the random sampling decided to make the contact discontinuity of $\mathbf{u_r}(.;\mathbf{u}_{j-1}^n,\mathbf{u}_j^n)$ enter the cell $\mathcal{C}_j$. Then we also have to account for the part of the solution $\mathbf{u_r}(.;\mathbf{u}_{j-1}^n,\mathbf{u}_j^n)$ located on the left of the contact discontinuity and entering the cell $\mathcal{C}_j$, that is equivalently the part of the solution $\mathbf{u_r}(.;\mathbf{u}_{j-1}^n,\mathbf{u}_j^{n+1/2})$ entering the cell $\mathcal{C}_j$.

Thus, by averaging on $[x_{j-1/2},x_j)$ as in (3.9) and since the condition $\mathbf{u}^\star(\mathbf{u}_{j-1}^n,\mathbf{u}_j^n)\neq\mathbf{u}_j^n$ is equivalent to $\mathbf{u}^\star(\mathbf{u}_{j-1}^n,\mathbf{u}_j^{n+1/2})\neq\mathbf{u}_j^{n+1/2}$ when $\mathbf{u}_j^{n+1/2}=\mathbf{u}_j^n$, we are thus led to set

$$\begin{aligned}\mathbf{u}_{j-1/2,R}^{n+1}&=\frac{2}{\Delta x}\int_{x_{j-1/2}}^{x_j}\mathbf{u_r}\left(\frac{x-x_{j-1/2}}{\Delta t};\mathbf{u}_{j-1}^n,\mathbf{u}_j^{n+1/2}\right)dx\\&=\mathbf{u}_j^{n+1/2}-\frac{2\Delta t}{\Delta x}\left(\mathbf{f}(\mathbf{u}_j^{n+1/2})-\mathbf{g}(\mathbf{u}_{j-1}^n,\mathbf{u}_j^{n+1/2})\right)\end{aligned}$$

$$\text{if}\quad \mathbf{u}^\star(\mathbf{u}_{j-1}^n,\mathbf{u}_j^{n+1/2})=\mathbf{u}_j^{n+1/2}, \tag{3.13}$$

$$\mathbf{u}_{j-1/2,R}^{n+1}=\frac{2}{\Delta x}\int_{x_{j-1/2}}^{x_j}\mathbf{u_r}\left(\frac{x-x_{j-1/2}}{\Delta t};\mathbf{u}_j^{n+1/2},\mathbf{u}_j^{n+1/2}\right)dx=\mathbf{u}_j^{n+1/2}$$

otherwise.

By (3.7), we get the following update formula :

$$\mathbf{u}_j^{n+1}=\frac{1}{2}(\mathbf{u}_{j+1/2,L}^{n+1}+\mathbf{u}_{j-1/2,R}^{n+1})=\mathbf{u}_j^{n+1/2}-\frac{\Delta t}{\Delta x}(\mathbf{g}_{j+1/2}^{n+1/2,L}-\mathbf{g}_{j-1/2}^{n+1/2,R})\ \text{for all } j\in\mathbb{Z}, \tag{3.14}$$

where the left and right numerical flux functions $\mathbf{g}_{j+1/2}^{n+1/2,L}$ and $\mathbf{g}_{j-1/2}^{n+1/2,R}$ are defined according to

$$\begin{aligned}&\mathbf{g}_{j+1/2}^{n+1/2,L}=\mathbf{g}(\mathbf{u}_j^{n+1/2},\mathbf{u}_{j+1}^n),\\&\text{and}\\&\mathbf{g}_{j-1/2}^{n+1/2,R}=\begin{cases}\mathbf{g}(\mathbf{u}_{j-1}^n,\mathbf{u}_j^{n+1/2}) & \text{if}\quad \mathbf{u}^\star(\mathbf{u}_{j-1}^n,\mathbf{u}_j^{n+1/2})=\mathbf{u}_j^{n+1/2},\\ \mathbf{f}(\mathbf{u}_j^{n+1/2}) & \text{otherwise.}\end{cases}\end{aligned} \tag{3.15}$$

The description of the method is now completed. Stability properties enjoyed by this algorithm are proposed below.

Remark 3. Putting the first and the second step together, we note that the definition of $\mathbf{u}_j^{n+1}$ only depends on $\mathbf{u}_{j-1}^n$, $\mathbf{u}_j^n$ and $\mathbf{u}_{j+1}^n$.

Remark 4. For numerical reasons, the test $\mathbf{u}^\star(\mathbf{u}_j^n,\mathbf{u}_{j+1}^{n+1/2})=\mathbf{u}_{j+1}^{n+1/2}$ in (3.15) is replaced with $|\mathbf{u}^\star(\mathbf{u}_j^n,\mathbf{u}_{j+1}^{n+1/2})-\mathbf{u}_{j+1}^{n+1/2}|\leq\epsilon$, with for instance $\epsilon=1.e^{-12}$.

THEOREM 3.1 (Consistency). *Under the CFL restriction (3.4), the scheme defined by (3.10)-(3.14)-(3.15) is consistent with (1.5) in the following sense :*
(i) Constant state : Assume that $\mathbf{u}:=\mathbf{u}_{j-1}^n=\mathbf{u}_j^n=\mathbf{u}_{j+1}^n$, *then* $\mathbf{u}_j^{n+1}=\mathbf{u}$.
(ii) Isolated contact discontinuity : Let $\mathbf{u}^l$ *and* $\mathbf{u}^r$ *be two distinct constant states that can be connected by a contact discontinuity. We set* $v:=v^l=v^r$. *Assume that* $\mathbf{u}_j^0=\mathbf{u}^l$ *if* $j\leq 0$ *and* $\mathbf{u}_j^0=\mathbf{u}^r$ *if* $j>0$. *Then the scheme (3.10)-(3.14)-(3.15) is equivalent to Glimm's random choice scheme and then converges to the solution of (2.2) given by*

$\mathbf{u}(x,t)=\mathbf{u}^l$ *if* $x<vt$ *and* $\mathbf{u}(x,t)=\mathbf{u}^r$ *otherwise. In particular, we have* $\mathbf{u}_j^n\in\{\mathbf{u}^l,\mathbf{u}^r\}$ $\forall\, j\in\mathbb{Z}$ *and* $\forall\, n\in\mathbb{N}$ *so that the velocity profile remains constant :* $v_j^n=v$ $\forall\, j\in\mathbb{Z}$ *and* $\forall\, n\in\mathbb{N}$.

(iii) Isolated 1-wave *: Let us assume that* $\mathbf{u}_{j-1}^n$ *and* $\mathbf{u}_j^n$ *can be connected by a* 1*-wave* $(\mathbf{u}^\star(\mathbf{u}_{j-1}^n,\mathbf{u}_j^n)=\mathbf{u}_j^n)$*. Then the definition* $\mathbf{u}_j^{n+1}$ *of our scheme (3.10)-(3.14)-(3.15) coincides with the one of the Godunov scheme, that is* $\mathbf{u}_j^{n+1}$ *is given by (3.2).* **Proof.**
(i) Let us assume that $\mathbf{u}_l^n=\mathbf{u}$ for $l=j-1,j,j+1$. Then, $\mathbf{u}^\star(\mathbf{u}_{j-1}^n,\mathbf{u}_j^n)=\mathbf{u}^\star(\mathbf{u},\mathbf{u})=\mathbf{u}$ and, by formula (3.10), we necessarily have $\mathbf{u}_j^{n+1/2}=\mathbf{u}$. Recall now the consistency property $\mathbf{g}(\mathbf{u},\mathbf{u})=\mathbf{f}(\mathbf{u})$ of the Godunov flux function. Invoking definition (3.15), we thus have

$$\mathbf{g}_{j+1/2}^{n+1/2,L}=\mathbf{g}(\mathbf{u},\mathbf{u})=\mathbf{f}(\mathbf{u})\quad\text{and}\quad\mathbf{g}_{j+1/2}^{n+1/2,R}=\mathbf{g}(\mathbf{u},\mathbf{u})=\mathbf{f}(\mathbf{u}).$$

Then, formula (3.14) proves that $\mathbf{u}_j^{n+1}=\mathbf{u}$.
(ii) Let us set $\mathbf{u}_j^0=\mathbf{u}^l$ if $j\leq 0$ and $\mathbf{u}_j^0=\mathbf{u}^r$ if $j>0$. Since $\mathbf{u}^l$ and $\mathbf{u}^r$ are assumed to be connected by a contact discontinuity, we have in particular $\mathbf{u}^\star(\mathbf{u}^l,\mathbf{u}^r)=\mathbf{u}^l$ (while of course $\mathbf{u}^\star(\mathbf{u}^l,\mathbf{u}^l)=\mathbf{u}^l$ and $\mathbf{u}^\star(\mathbf{u}^r,\mathbf{u}^r)=\mathbf{u}^r$) so that the definition of $\mathbf{u}_j^{n+1/2}$ in (3.10) coincides with the one provided by the Glimm scheme. To prove our result, we thus have to show that $\mathbf{u}_j^{n+1}=\mathbf{u}_j^{n+1/2}$. The two situations of interest are first $\mathbf{u}_k^{n+1/2}=\mathbf{u}^l$ for $k\leq j$ and $\mathbf{u}_k^{n+1/2}=\mathbf{u}^r$ otherwise, and then $\mathbf{u}_k^{n+1/2}=\mathbf{u}^l$ for $k<j$ and $\mathbf{u}_k^{n+1/2}=\mathbf{u}^r$ otherwise.
In the first situation, we necessarily have $\mathbf{u}_{j-1}^n=\mathbf{u}^l$ (respectively $\mathbf{u}_{j+1}^n=\mathbf{u}^r$) since otherwise we would have $\mathbf{u}_{j-1}^n=\mathbf{u}_j^n=\mathbf{u}^r$ and then $\mathbf{u}_j^{n+1/2}=\mathbf{u}^r$ (respectively $\mathbf{u}_j^n=\mathbf{u}_{j+1}^n=\mathbf{u}^l$ and then $\mathbf{u}_{j+1}^{n+1/2}=\mathbf{u}^l$). Then we have $\mathbf{g}_{j+1/2}^{n+1/2,L}=\mathbf{g}(\mathbf{u}^l,\mathbf{u}^r)=\mathbf{f}(\mathbf{u}^l)$ because the contact discontinuity propagates to the right-hand side. Moreover, $\mathbf{g}_{j-1/2}^{n+1/2,R}=\mathbf{g}(\mathbf{u}^l,\mathbf{u}^l)=\mathbf{f}(\mathbf{u}^l)$, so that $\mathbf{u}_j^{n+1}=\mathbf{u}_j^{n+1/2}$ by (3.14).
In the second situation, we note that $\mathbf{u}_{j+1}^n=\mathbf{u}^r$, since otherwise we would have $\mathbf{u}_j^n=\mathbf{u}_{j+1}^n=\mathbf{u}^l$ and then $\mathbf{u}_j^{n+1/2}=\mathbf{u}^l$. Hence $\mathbf{g}_{j+1/2}^{n+1/2,L}=\mathbf{g}(\mathbf{u}^r,\mathbf{u}^r)=\mathbf{f}(\mathbf{u}^r)$. As far as $\mathbf{g}_{j-1/2}^{n+1/2,R}$ is concerned
- either $\mathbf{u}_{j-1}^n=\mathbf{u}^l$ and then $\mathbf{u}^\star(\mathbf{u}_{j-1}^n,\mathbf{u}_j^{n+1/2})=\mathbf{u}^\star(\mathbf{u}^l,\mathbf{u}^r)=\mathbf{u}^l\neq\mathbf{u}^r$, which means $\mathbf{g}_{j-1/2}^{n+1/2,R}=\mathbf{f}(\mathbf{u}^r)$ by (3.15),
- or $\mathbf{u}_{j-1}^n=\mathbf{u}^r$ and then $\mathbf{u}^\star(\mathbf{u}_{j-1}^n,\mathbf{u}_j^{n+1/2})=\mathbf{u}^\star(\mathbf{u}^r,\mathbf{u}^r)=\mathbf{u}^r$, which means again $\mathbf{g}_{j-1/2}^{n+1/2,R}=\mathbf{f}(\mathbf{u}^r)$ by (3.15).
The two fluxes $\mathbf{g}_{j+1/2}^{n+1/2,L}$ and $\mathbf{g}_{j-1/2}^{n+1/2,R}$ then coincide and equality $\mathbf{u}_j^{n+1}=\mathbf{u}_j^{n+1/2}$ follows.
We have thus proved that the second step of the algorithm is transparent, which means that the method reduces to the first step and it is equivalent to Glimm's random choice scheme. The convergence towards the solution $\mathbf{u}(x,t)=\mathbf{u}^l$ for $x<vt$ and $\mathbf{u}(x,t)=\mathbf{u}^r$ for $x>vt$ is proved in [18] (see also [22]) as soon as the random sequence (a_n) is well distributed.
(iii) If $\mathbf{u}_{j-1}^n$ and $\mathbf{u}_j^n$ can be connected by a 1-wave, we have $\mathbf{u}^\star(\mathbf{u}_{j-1}^n,\mathbf{u}_j^n)=\mathbf{u}_j^n$ and then $\mathbf{u}_j^{n+1/2}=\mathbf{u}_j^n$. Hence, by definition (3.15), we have $\mathbf{g}_{j+1/2}^{n+1/2,L}=\mathbf{g}(\mathbf{u}_j^n,\mathbf{u}_{j+1}^n)=\mathbf{f}_{j+1/2}^n$ and $\mathbf{g}_{j-1/2}^{n+1/2,R}=\mathbf{g}(\mathbf{u}_{j-1}^n,\mathbf{u}_j^n)=\mathbf{f}_{j-1/2}^n$. Then the definition of $\mathbf{u}_j^{n+1}$ given by our scheme (3.10)-(3.14)-(3.15) coincides with the one of the Godunov scheme, that is $\mathbf{u}_j^{n+1}$ is

given by (3.2). This completes the proof of the theorem. □

THEOREM 3.2 (Maximum principle). *Under the CFL restriction (3.4), the scheme defined by (3.10)-(3.14)-(3.15) satisfies the following maximum principle property for all $j \in \mathbb{Z}$ and all $n \in \mathbb{N}$:*

$$\begin{cases} \inf\limits_{j\in\mathbb{Z}} v_j^0 \le v_j^n \le \sup\limits_{j\in\mathbb{Z}} v_j^0, \\ \inf\limits_{j\in\mathbb{Z}} (v_j^0 + p(\rho_j^0)) \le v_j^n + p(\rho_j^n) \le \sup\limits_{j\in\mathbb{Z}} (v_j^0 + p(\rho_j^0)). \end{cases}$$

Proof.
Maximum principle is not affected by the first step since for all $j \in \mathbb{Z}$, $\mathbf{u}_j^{n+1/2}$ is defined by picking up randomly a value between $\mathbf{u}^\star(\mathbf{u}_{j-1}^n, \mathbf{u}_j^n)$ and $\mathbf{u}_j^n$. Since in each Riemann solution one has $v + p(\rho) = \text{const}$ and $v = \text{const}$ along the first wave and the second wave respectively, we then obtain

$$\inf\{v_{j-1}^n + p(\rho_{j-1}^n), v_j^n + p(\rho_j^n)\} \le v_j^{n+1/2} + p(\rho_j^{n+1/2}) \le \sup\{v_{j-1}^n + p(\rho_{j-1}^n), v_j^n + p(\rho_j^n)\}$$

and

$$v_j^{n+1/2} = v_j^n.$$

Concerning the second step, new values are introduced in cells $\mathcal{C}_j$ taking averages of (parts of) Riemann solutions containing only waves of the first family, namely $\mathbf{u_r}(.; \mathbf{u}_j^{n+1/2}, \mathbf{u}_{j+1}^n)$ on $[x_j, x_{j+1/2})$, and $\mathbf{u_r}(.; \mathbf{u}_{j-1}^n, \mathbf{u}_j^{n+1/2})$ or $\mathbf{u_r}(.; \mathbf{u}_j^{n+1/2}, \mathbf{u}_j^{n+1/2})$ on $[x_{j-1/2}, x_j)$. Since again $v + p(\rho) = \text{const} = C$ along these waves, and therefore $y = \rho C$, we get $y_j^{n+1} = \rho_j^{n+1} C_j^{n+1/2} = \rho_j^{n+1}(v_j^{n+1/2} + p(\rho_j^{n+1/2}))$, so that $v_j^{n+1} + p(\rho_j^{n+1}) = C_j^{n+1/2} = v_j^{n+1/2} + p(\rho_j^{n+1/2})$. The maximum principle property thus holds for $v + p(\rho)$. We now calculate the velocity v_j^{n+1} using formula

$$v_j^{n+1} = \frac{y_j^{n+1}}{\rho_j^{n+1}} - p(\rho_j^{n+1}) = C_j^{n+1/2} - p(\rho_j^{n+1}).$$

Let us note ρ^- (respectively ρ^+) the min (respectively max) value of ρ among all the states involved in the averaging procedure of the second step and v^- (respectively v^+) the corresponding velocity. Since the function p is monotone (increasing) we get

$$\inf\{v_{j-1}^n, v_j^{n+1/2} = v_j^n, v_{j+1}^n\} \le v^+ \le v_j^{n+1} \le v^- \le \sup\{v_{j-1}^n, v_j^{n+1/2} = v_j^n, v_{j+1}^n\}$$

and the maximum principle property also holds for v. □

Remark 5. The present algorithm is consistent with (1.5) in the sense of Theorem 3.1 and obeys a maximum principle property on both Riemann invariants $v + p(\rho)$ and v. By the latter property, contact discontinuities are properly computed (without oscillations), as it is clearly shown in the next section. The counterpart is that our method is no longer conservative on the density and the momentum, even if the conservation errors are really small (see again the next section). Instead of averaging ρ and y as in the usual Godunov method, a way to properly capture the contact discontinuities while still being conservative on ρ would be to average the density ρ and the velocity v. However, the difficulty would be to obtain a simple form of the corresponding update formula since v is not a conservative variable for general pressure laws, as well as a maximum principle property on $v + p(\rho)$.

Remark 6 (Computational cost). According to (3.14), the definition of $\mathbf{u}_j^{n+1}$ relies on the computation of the time intermediate value $\mathbf{u}_j^{n+1/2}$ and two numerical fluxes $\mathbf{g}_{j+1/2}^{n+1/2,L}$ and $\mathbf{g}_{j-1/2}^{n+1/2,R}$. The computation of $\mathbf{u}_j^{n+1/2}$ is generally associated with the computation of $\mathbf{u}^\star(\mathbf{u}_{j-1}^n,\mathbf{u}_j^n)$ by (3.10), while the computation of $\mathbf{g}_{j+1/2}^{n+1/2,L}$ and $\mathbf{g}_{j-1/2}^{n+1/2,R}$ corresponds in general to the computation of two Godunov fluxes by (3.15), namely $\mathbf{g}(\mathbf{u}_j^{n+1/2},\mathbf{u}_{j+1}^n)$ and $\mathbf{g}(\mathbf{u}_{j-1}^n,\mathbf{u}_j^{n+1/2})$. It is clear that the computation of $\mathbf{u}^\star(\mathbf{u}_{j-1}^n,\mathbf{u}_j^n)$ is part of the computation of the Godunov flux $\mathbf{g}(\mathbf{u}_j^{n+1/2},\mathbf{u}_{j+1}^n)$. Hence the definition of $\mathbf{u}_j^{n+1}$ is eventually associated with the computation of two Godunov fluxes instead of one as in the usual Godunov method (since it is conservative). This additional cost is usual when trying to properly compute contact discontinuities, see [2] for instance. However, the computation of a Godunov flux is not expensive for the system under consideration in this paper (see Section 2).

4. Numerical experiments

Let us first recall that in this section, p is given definition (1.3). We will take $R=1$ and $v_{ref}=1.4427$. In order to test the proposed scheme, we consider three Riemann problems leading to three solutions of interest: an isolated contact discontinuity (Test 1), a shock wave followed by a contact discontinuity (Test 2) and a sonic rarefaction wave followed by a contact discontinuity (Test 3). In each case, the method is first evaluated by means of a qualitative comparison with the exact solution: the ρ, v and $v+p(\rho)$ profiles are shown on Figures 4.1, 4.2 and 4.3. For several mesh sizes, a quantitative evaluation through the L^1-norm (of the difference between the exact and numerical solutions) is then made, as well as a measure of the conservation errors on both ρ and y. They are given on tables 4.1, 4.2, 4.3 : E^ρ_{cons} and E^y_{cons} denote the conservation errors on ρ and y, and $E^\rho_{L^1}$ and $E^v_{L^1}$ denote the L^1-errors on ρ and v. The L^1-norm errors are computed in a very classical way. For the sake of completeness, we now give the precise meaning of E^ρ_{cons} and E^y_{cons} in our computations (and we refer for instance the reader to [2], [5], [6] for more details on these formulas) : denoting $[x_0,x_1]=[-0.25,0.75]$ the computational domain of our simulations and T_f the corresponding final time, we first set for all $n\geq 0$

$$E^{\mathbf{u}}(t^n)=\begin{pmatrix}E^\rho(t^n)\\ E^y(t^n)\end{pmatrix}$$
$$=\frac{\displaystyle\int_{x_0}^{x_1}\mathbf{u}_\nu(x,t^n)dx-\int_{x_0}^{x_1}\mathbf{u}_\nu(x,0)dx+\int_0^{t^n}\mathbf{f}(\mathbf{u}_\nu(x_1,s))ds-\int_0^{t^n}\mathbf{f}(\mathbf{u}_\nu(x_0,s))ds}{\displaystyle\int_{x_0}^{x_1}\mathbf{u}_\nu(x,t^n)dx}$$

where the ratio has to be understood component by component, and then

$$E^{\mathbf{u}}_{cons}=\begin{pmatrix}E^\rho_{cons}\\ E^y_{cons}\end{pmatrix}=\frac{1}{T_f}\sum_{n=0}^{N}\Delta t|E^{\mathbf{u}}(t^n)|\qquad\text{with } N=T_f/\Delta t.$$

Note that $\mathbf{u}_\nu$ being piecewise constant, these quantities are easy to evaluate. Note also that $E^{\mathbf{u}}_{cons}$ corresponds to the sum of the absolute value of the relative conservation errors made at each intermediate time t^n. In other words, the possible compensation effects are not taken into account here.

Initial states are chosen as follows:

Test 1			**Test 2**			**Test 3**		
$\mathbf{u}^l$:	$\rho^l = 0.9$	$v^l = 1.$	$\mathbf{u}^l$:	$\rho^l = 0.1$	$v^l = 1.8$	$\mathbf{u}^l$:	$\rho^l = 0.5$	$v^l = 1.2$
$\mathbf{u}^r$:	$\rho^r = 0.1$	$v^r = 1.$	$\mathbf{u}^r$:	$\rho^r = 0.2$	$v^r = 1.6$	$\mathbf{u}^r$:	$\rho^r = 0.1$	$v^r = 1.6$

The qualitative results are presented on a mesh made of 100 points per unit interval.

We observe as predicted above that the classical Godunov method develops spurious oscillations near the contact discontinuity, that strongly affect the whole numerical solution[1]. On the contrary, our algorithm removes them and provides numerical solutions in full agreement with exact ones, and with sharp contact discontinuities. As far as the conservation errors and the L^1-errors are concerned, they tend to zero with the mesh size, which proves numerically the convergence of the method. Moreover, we see that the L^1-errors between the numerical and exact solutions are really lower for our scheme compared with the Godunov method.

# of points	E^{ρ}_{cons}	E^{y}_{cons}	$E^{\rho}_{L^1}$	$E^{v}_{L^1}$
100	0.	0.	$8.39e^{-2}$	$8.68e^{-2}$
500	0.	0.	$4.26e^{-2}$	$3.83e^{-2}$
1000	0.	0.	$3.06e^{-2}$	$2.66e^{-2}$
2000	0.	0.	$2.18e^{-2}$	$1.85e^{-2}$

# of points	E^{ρ}_{cons}	E^{y}_{cons}	$E^{\rho}_{L^1}$	$E^{v}_{L^1}$
100	1.52%	7.74%	$8.e^{-3}$	0.
500	0.32%	1.83%	$1.6e^{-3}$	0.
1000	0.16%	0.94%	$8.e^{-4}$	0.
2000	0.08%	0.47%	$4.e^{-4}$	0.

TABLE 4.1. **Test 1** *: Godunov scheme (top) and our scheme (bottom).*

5. Conclusion

We have presented an algorithm whose objective is to remove the spurious oscillations generated by the Godunov scheme near contact discontinuities in the Aw-Rascle model for traffic flow. The method proposes to treat separately the contact discontinuities using a random sampling strategy, and to keep on using the Godunov scheme for the other waves. The whole algorithm is not strictly conservative but numerical experiments give very good numerical solutions with *sharp* (*i.e.* without numerical diffusion nor oscillations) contact discontinuities and small conservation errors, and show the numerical convergence. Moreover, we are able to prove that the method enjoys important stability properties like strong consistency and maximum principle on the Riemann invariants of the system.

The resulting scheme remains dependent on the exact Riemann solver. Even if

[1] We also observe that the spurious oscillations are mainly located behind the contact discontinuity. The reason which can explain this fact is probably that, in any given Riemann problem, the wave which propagates with the largest velocity is precisely the contact discontinuity (the other waves are then located behind the contact discontinuity).

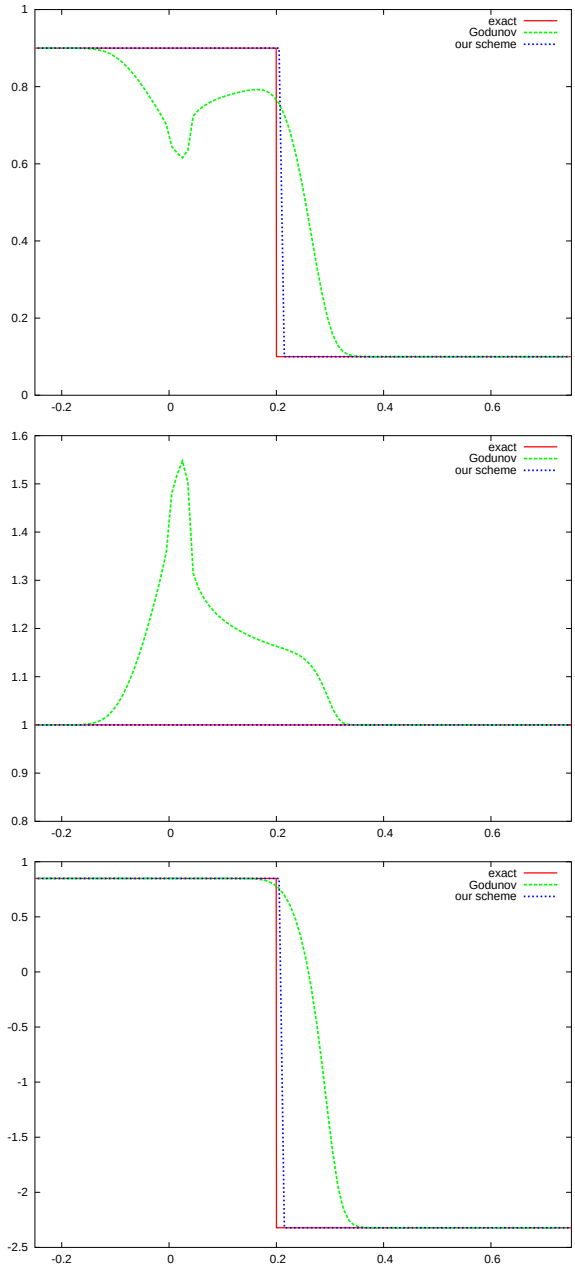

FIG. 4.1. **Test 1** : *ρ (Left), v (Right) and $v+p(\rho)$ (Bottom) at time $t=0.2$.*

its use is very cheap in this case, it would be interesting in perspective to observe how our strategy behaves when the exact Riemann solver is replaced by an approximate Riemann solver.
Another important topic would be the extension of the presented approach to higher-order schemes.

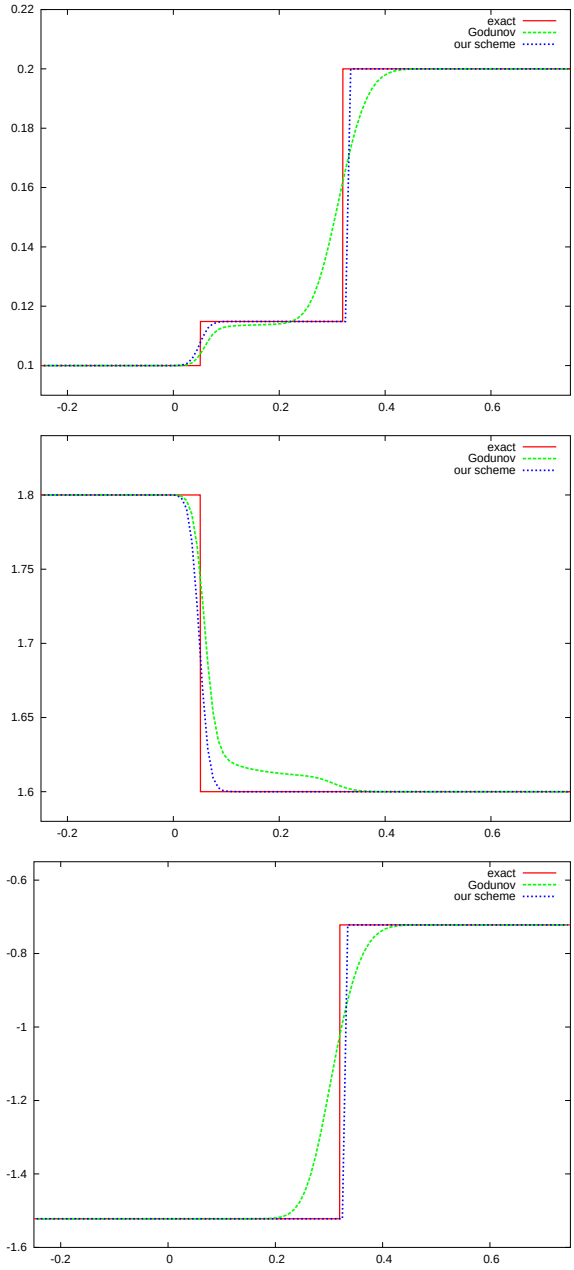

FIG. 4.2. **Test 2** : *ρ (Left), v (Right) and $v+p(\rho)$ (Bottom) at time $t=0.2$.*

REFERENCES

[1] R. Abgrall. How to prevent pressure oscillations in multicomponent flow calculations: a quasi-conservative approach. *J. Comput. Phys.*, 125:150–160, 1996.

[2] R. Abgrall and S. Karni. Computations of compressible multifluids. *J. Comput. Phys.*, 169:594–623, 2001.

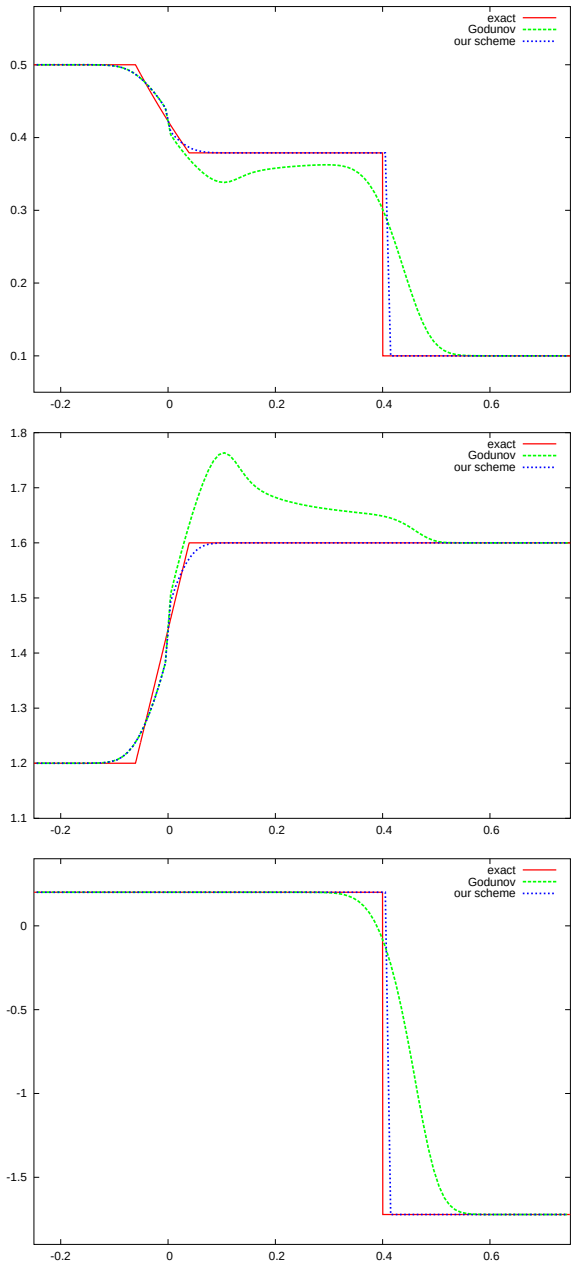

FIG. 4.3. **Test 3** : *ρ (Left), v (Right) and $v+p(\rho)$ (Bottom) at time $t=0.25$.*

[3] A. Aw and M. Rascle. Resurrection of "second order" models of traffic flow. *SIAM J. Appl. Math.*, 60:916–938, 2000.

[4] T. Barberon, P. Helluy, and S. Rouy. Practical computation of axisymmetrical multifluid flows. *International Journal of Finite Volumes*, 1:1–34, 2003.

[5] C. Chalons. Transport-equilibrium schemes for computing nonclassical shocks. scalar conservation laws. Preprint, available at http://www.math.ntnu.no/conservation/2006/051.html,

# of points	E^{ρ}_{cons}	E^{y}_{cons}	$E^{\rho}_{L^1}$	$E^{v}_{L^1}$
100	0.	0.	$3.2e^{-3}$	$6.55e^{-3}$
500	0.	0.	$1.47e^{-3}$	$2.76e^{-3}$
1000	0.	0.	$1.03e^{-3}$	$1.78e^{-3}$
2000	0.	0.	$7.3e^{-4}$	$1.22e^{-3}$

# of points	E^{ρ}_{cons}	E^{y}_{cons}	$E^{\rho}_{L^1}$	$E^{v}_{L^1}$
100	0.35%	0.14%	$1.02e^{-3}$	$2.3e^{-3}$
500	0.07%	0.03%	$2.19e^{-4}$	$6.47e^{-4}$
1000	0.04%	0.02%	$1.09e^{-4}$	$3.26e^{-4}$
2000	0.03%	0.01%	$9.72e^{-5}$	$1.63e^{-4}$

TABLE 4.2. **Test 2** *: Godunov scheme (top) and our scheme (bottom).*

# of points	E^{ρ}_{cons}	E^{y}_{cons}	$E^{\rho}_{L^1}$	$E^{v}_{L^1}$
100	0.	0.	$2.12e^{-2}$	$3.8e^{-2}$
500	0.	0.	$9.82e^{-3}$	$1.68e^{-2}$
1000	0.	0.	$6.98e^{-3}$	$1.17e^{-2}$
2000	0.	0.	$4.94e^{-3}$	$8.22e^{-3}$

# of points	E^{ρ}_{cons}	E^{y}_{cons}	$E^{\rho}_{L^1}$	$E^{v}_{L^1}$
100	0.81%	6.04%	$3.82e^{-3}$	$3.36e^{-3}$
500	0.17%	1.14%	$9.41e^{-4}$	$1.25e^{-3}$
1000	0.08%	0.57%	$5.17e^{-4}$	$7.78e^{-4}$
2000	0.04%	0.28%	$2.84e^{-4}$	$4.72e^{-4}$

TABLE 4.3. **Test 3** *: Godunov scheme (top) and our scheme (bottom).*

2006.

[6] C. Chalons. Numerical approximation of a macroscopic model of pedestrian flows. *SIAM J. Sci. Comput.*, 2007.

[7] C. Chalons and F. Coquel. Numerical contact discontinuities in single fluid and multifluid computations. Preprint.

[8] C. Chalons and P. Goatin. Godunov scheme and sampling technique for computing phase transitions in traffic flow modeling. Preprint, available at http://www.math.ntnu.no/conservation/2006/052.html, 2006.

[9] P. Collela. Glimm's method for gas dynamics. *SIAM J. Sci. Stat. Comput.*, 3:76–110, 1982.

[10] R. M. Colombo. A 2×2 hyperbolic traffic flow model. *Math. Comput. Modeling*, 35(5-6):683–688, 2002.

[11] R. M. Colombo. Hyperbolic phase transitions in traffic flow. *SIAM J. Appl. Math.*, 63(2):708–721, 2002.

[12] C. F. Daganzo. Requiem for high-order fluid approximations of traffic flow. *Trans. Res.*, 29B(4):277–287, August 1995.

[13] R. P. Fedkiw, T. Aslam, B. Merriman, and S. Osher. A non-oscillatory eulerian approach to interfaces in multimaterial flows (the ghost fluid method). *J. Comput. Phys.*, 152:457–492, 1999.

[14] P. Goatin. The Aw-Rascle traffic flow model with phase transition. *Math. Comput. Modeling.*, 44:287–303, 2006.

[15] S. Karni. Multicomponent flow calculations by a consistent primitive algorithm. *J. Comput. Phys.*, 47:1115–1145, 1994.

[16] S. Karni. Hybrid multifluid algorithms. *SIAM J. Sci. Comput.*, 17:1019–1039, 1996.

[17] M. J. Lighthill and G. B. Whitham. On kinematic waves. II. A theory of traffic flow on long crowded roads. *Proc. Roy. Soc. London. Ser. A.*, 229:317–345, 1955.

[18] T. P. Liu. The deterministic version of the Glimm scheme. *Comm. Math. Phys.*, 57:135–148, 1977.

[19] H. J. Payne. Models of freeway traffic and control. In *Simulation Council Proc.28*, pages 51–61. Math. Models Publ. Sys., 1971.

[20] P. I. Richards. Shock waves on the highway. *Operations Res.*, 4:42–51, 1956.

[21] R. Saurel and R. Abgrall. A simple method for compressible multifluid flows. *SIAM J. Sci. Comput.*, 21:1115–1145, 1999.

[22] D. Serre. *Systèmes de lois de conservation.* Diderot éditeur, Arts et Sciences, 1996.

[23] B. Temple. Systems of conservation laws with coinciding shock and rarefaction curves. *Contemp. Math.*, 17:143–151, 1983.

[24] G. B. Whitham. *Linear and Nonlinear Waves.* John Wiley and Sons, New York, 1999.